World Journal of
Chemical and Pharmaceutical Sciences

Journal homepage: https://zealjournals.com/wjcps/

ISSN: 2945-3186 (Online)

(RESEARCH ARTICLE)

Check for updates

Synthesis, characterization, and antibacterial activity of Benzimidazole Schiff Bases and Bis(thiazolidin-4-one) Derivatives

Fatima Abdulkareem Eraibi *

College of Pharmacy, University of Tikrit.

World Journal of Chemical and Pharmaceutical Sciences, 2026, 09(01), 026–040

Publication history: Received on 07 June 2026; revised on 14 July 2026; accepted on 16 July 2026

Article DOI: https://doi.org/10.53346/wjcps.2026.9.1.0023

Abstract

A sequential synthetic route was developed for the preparation of benzimidazole-linked Schiff bases and bis(thiazolidin-4-one) derivatives. 4-(1H-Benzimidazol-2-yl)aniline (H1) was obtained by acid-promoted cyclocondensation of o-phenylenediamine with 4-aminobenzoic acid. Condensation of H1 with 4-aminoacetophenone afforded the mono-Schiff base H2 while retaining a free para-amino group. Subsequent reactions of H2 with 4-methylbenzaldehyde and 4-bromobenzaldehyde yielded the bis-Schiff bases H3 and H4, respectively. Cyclization of H3 and H4 with thioglycolic acid in the presence of anhydrous zinc chloride produced the corresponding bis(thiazolidin-4-one) derivatives H5 and H6. The structures were evaluated using FTIR and NMR spectroscopy. Schiff-base formation was supported by the appearance of imine-related signals and the disappearance of the residual amino-group pattern after the second condensation, whereas ring closure was evidenced by thiazolidinone carbonyl absorptions and new aliphatic resonances assigned to the five-membered rings. Antibacterials activity is evaluate by the agar well diffusions method against *Escherichia coli* and *Staphylococcus aureus*. The cyclize derivatives H5 and H6 produced larger inhibitions zones than their Schiff-base precursors, and H6 showed the greatest activition, with inhibition-zone diameters of 24 and 26 mm against *E. coli* and *S. aureus*, respectively. These findings indicate that thiazolidin-4-one ring formation and the para-bromo substituent enhance the antibacterial response within the investigated series.

Keywords: Benzimidazole; Schiff Base; Thiazolidin-4-One; Thioglycolic Acid; FTIR; NMR Spectroscopy; Antibacterial Activity; Agar Well Diffusion

1. Introduction

Benzimidazole was a privileged fuse nitrogen heterocycle who electronic versatility, hydrogen-bonding capacities, and compatibility with diverse substituents made it a productive platform for molecular design. Recently studies has demonstrated that benzimidazole frameworks can be integrated with imine linkage to generated structurally tunable hybrid with extended conjugation and readily modifiable donor sites [1]. Such hybrids has also been investigated as multitarget molecular systems, illustrating how a benzimidazole nucleus can served simultaneously as a recognition unit and as a scaffold for further functionalization [2]. Benzylidene-amino benzimidazoles provided a particularly direct examples of this strategy because the imine bonds connects two aromatic domains while preserving synthetic accessibility [3]. Coordination studies of Schiff base further show that the C=N unit can alter electronic distributions, metal-bind behavior, and spectroscopic responses [4].

The continue interest in benzimidazole-contain hybrid is also linked to the efficiency with structurally distinct pharmacophore can joined in a single molecular architecture. Benzimidazole-triazole systems have recently has been prepare and characterized as compact heterocyclic hybrid [5], while benzimidazole, thiazolidin-4-one combinations has shown that a fuse N-heterocycle was successful merged with sulfur- and oxygen-containing five-membered rings [6]. Imine ligand derive from benzimidazole has likewise been characterized by vibrational, nuclear magnetic resonance,

* Corresponding author: Fatima Abdulkareem Eraibi

and computational method, emphasize the importance of convergent analytical evidence when assigned these structural [7]. These reports collectively support the used of benzimidazole-linked Schiff base as synthetically useful intermediate rather than merely finally productions.

The thiazolidin-4-ones constitute another wide explore heterocyclic class. Their prepare commonly relies on cyclocondensation of an imine with a mercapto carboxylic acid, a transformation that converts a planar C=N linkage in a saturate N-C-S ring bear a diagnostic carbonyl groups. Recent thiazolidin-4-one series containing oxadiazole or thiadiazole units have been authenticated by FTIR, NMR, mass spectrometry, and elemental analysis [8]. Related studies have combined experimental characterization with molecular modeling to establish substitution-dependent structure-property relationships [9]. Phenylaminopyrimidine-thiazolidinone hybrids [10], indole-thiazole/thiazolidinone systems [11], and ester-linked thiazolidinone derivatives [12] illustrate the broad tolerance of this ring-forming reaction toward aromatic and heteroaromatic precursors.

The imine-to-thiazolidinone sequence is attractive because the two stages provide complementary spectroscopic markers. Schiff-base formation is generally associated with loss of the precursor carbonyl or amino signatures and appearance of C=N-related bands and resonances, whereas ring closure introduces a lactam-type C=O absorption and characteristic aliphatic signals from the thiazolidinone ring. Contemporary Schiff-base studies combine these markers with computational or biological evaluation [13], and substituted thiazolidinones continue to be investigated as modular heterocyclic systems [14]. The influence of aryl substitution has been examined in halogenated and electron-donating analogues, where changes in electronic and steric environment affect both spectral positions and downstream properties [15]. Recent synthetic methods to 4-thiazolidinones has also emphasize the value of clear mechanistic and spectra differentiation between imine precursor and cyclize productions [16].

Match recently investigation has expanded thiazolidinone chemistry to enzyme-direct thiazole-thiazolidinone hybrid [17], carvone-linke triazole-thiazolidinones [18], and aminothiazole-base multifunctional molecules [19]. Sustainable approaches, including deep eutectic solvents, have also been explored for thiazolidinone formation [20], while indole-derived thiazolidinones demonstrate the broad compatibility of this ring system with different aromatic scaffolds [21]. Contemporary benzimidazole studies continue to rely on FTIR and multinuclear NMR spectroscopy for reliable structural assignment [22]. In parallel, benzimidazole, Schiff-base, halogenated, and thiazolidin-4-one motifs have been associated with antibacterial activity [4,6,8,13,15]. Accordingly, the present study aimed to synthesize the sequential series H1–H6, characterize the structural changes accompanying imine formation and thiazolidin-4-one ring closure, and evaluate the antibacterial activity of the prepared compounds against *Escherichia coli* and *Staphylococcus aureus*.

2. Experimental method

2.1. Materials and instrumentation

All reagents and solvents were of analytical grade and were used without further purification unless otherwise stated. FTIR spectra were recorded over the range 4000–400 cm^{-1} using KBr pellets on a Shimadzu FTIR-8400S spectrometer. Melting points were determined using a Stuart melting-point apparatus and are uncorrected. ^{1}H and ^{13}C NMR spectra were recorded on a Bruker 400 MHz spectrometer at 400 and 100 MHz, respectively. DMSO-d_6 was used as the solvent, and chemical shifts are reported in parts per million relative to the residual solvent signals. Reaction progress was monitored by thin-layer chromatography on silica gel plates.

2.2. Synthesis of 4-(1H-benzimidazol-2-yl)aniline (H1)

Following a reported procedure with minor modification [23], o-phenylenediamine (0.01 mol) and 4-aminobenzoic acid (0.01 mol) were combined in 4 M hydrochloric acid (20 mL) and heated under reflux for 30 min. After cooling, the formed solid was collected by filtration, washed, dried, and recrystallized from absolute ethanol to afford H1.

2.3. Synthesis of 4-[1-({4-(1H-benzimidazol-2-yl)phenyl}imino)ethyl]aniline (H2)

Equimolar quantities of H1 (0.01 mol) and 4-aminoacetophenone (0.01 mol) were refluxed in ethanol (20 mL) for 2 h. The reaction mixture was cooled and allowed to stand for 24 h. The crystalline product was collected by filtration, dried, and recrystallized from ethanol to give H2.

2.4. General synthesis of the bis-Schiff bases H3 and H4

H2 (0.01 mol) and the appropriate aromatic aldehyde (0.01 mol; 4-methylbenzaldehyde for H3 or 4-bromobenzaldehyde for H4) were refluxed in ethanol (30 mL) for 20 min. After cooling, each reaction mixture was

allowed to stand for 24 h. The resulting crystalline product was collected by filtration, dried, and recrystallized from ethanol to afford H3 or H4.

2.5. General synthesis of the bis(thiazolidin-4-one) derivatives H5 and H6

The cyclization procedure was adapted from a reported thiazolidinone synthesis [24]. The corresponding bis-Schiff base H3 or H4 (0.001 mol) and thioglycolic acid (0.002 mol) were dissolved in 1,4-dioxane (20 mL). Anhydrous zinc chloride (0.7 g) was added, and the reaction mixture was heated under reflux for 8 h. After cooling, the precipitated product was collected, washed with aqueous sodium bicarbonate to remove residual acid, and recrystallized from absolute ethanol. Cyclization of H3 afforded H5, whereas cyclization of H4 afforded H6.

2.6. Physical properties

The physical properties of compounds H1–H6 are summarized in Table 1.

Table 1 Physical properties of compounds H1–H6.

Compound	Color	Melting point (°C)	Yield (%)
H1	Pale yellow	209–211	76.9
H2	Purple	220	94.1
H3	Golden yellow	160–165 (dec.)	46–55
H4	Brown	145–155 (dec.)	35–45
H5	Brown	198–202	60–65
H6	Dark brown	202–206	58–63

2.7. Antibacterial activity study

Antibacterial activation of compounds H1–H6 was evaluate use the agar well diffusions method against *Escherichia coli* and *Staphylococcus aureus*. Nutrient agar is prepare by dissolve 37.5 g of the medium in 1.0 L of water, adjusting the pH to 7.3, sterilize at 121 °C for 15 min, and dispensed 20–25 mL into sterile Petri dishes.

Bacterially suspensions are prepared from fresh colonies in sterile physiological saline (0.85% NaCl). The turbidity was adjust to the 0.5 McFarland standard, corresponded to approximately 1.5×10^8 CFU/mL, and each suspension is spread uniformly over the agar surfaces use a sterile glass spreader.

Solution of compounds H1–H6 are prepare in DMSO at concentrationsof 10 mg/mL. Wells of 6 mm diameter are make using a sterile cork borer, and 100 µL of each solutions, equivalent to 1 mg per well, is add. DMSO was used as the negative control. The plates are maintained at 4 °C for 30 min to permit diffusion and are then incubated at 37 °C for 24 h. Antibacterial activity is expressed as the measured inhibition-zone diameter in millimeters.

3. Results and Discussion

3.1. Synthetic Route of Compounds H1–H6

The synthesis of compounds H1–H6 commenced with the preparation of 4-(1H-benzimidazol-2-yl)aniline (H1) through the cyclocondensation of o-phenylenediamine with 4-aminobenzoic acid in hydrochloric acid. This was followed by the condensation of H1 with 4-aminoacetophenone to afford the mono-Schiff base H2, which retained a free para-amino group. Subsequently, H2 was reacted with 4-methylbenzaldehyde or 4-bromobenzaldehyde to yield the corresponding bis-Schiff bases H3 and H4, respectively. Finally, cyclization of H3 and H4 with thioglycolic acid in the presence of anhydrous zinc chloride produced the bis(thiazolidin-4-one) derivatives H5 and H6. The overall synthetic route and the prepared compounds are presented in Scheme 1.

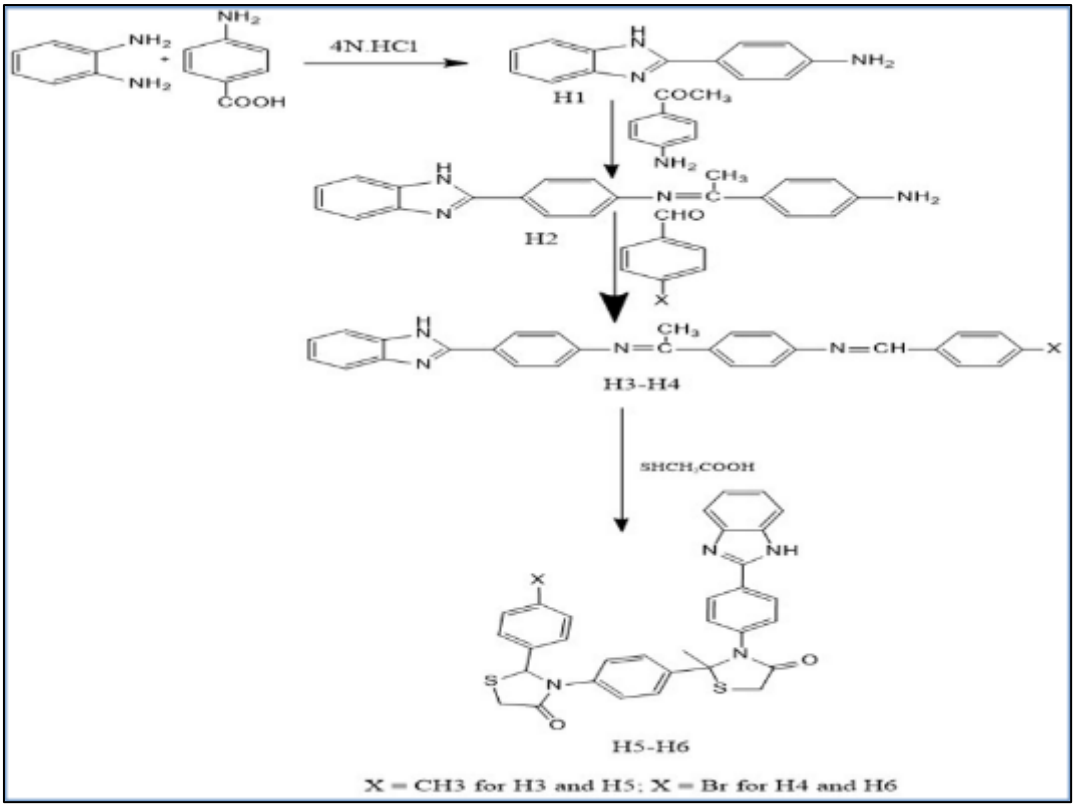

Scheme 1 Synthetic route to compounds H1–H6.

The systematic names, molecular formulas, and molar masses of the synthesized compounds H1–H6 are summarized in Table 2.

Table 2 Systematic names, molecular formulas, and calculated molar masses of compounds H1–H6.

Comp.	Systematic name	Molecular formula	Molar mass (g mol^{-1})
H1	4-(1H-Benzimidazol-2-yl)aniline	$C_{13}H_{11}N_3$	209.25
H2	4-[1-({4-(1H-benzimidazol-2-yl)phenyl}imino)ethyl]aniline	$C_{21}H_{18}N_4$	326.40
H3	4-[1-({4-(1H-benzimidazol-2-yl)phenyl}imino)ethyl]-N-(4-methylbenzylidene)aniline	$C_{29}H_{24}N_4$	428.54
H4	N-(4-Bromobenzylidene)-4-[1-({4-(1H-benzimidazol-2-yl)phenyl}imino)ethyl]aniline	$C_{28}H_{21}BrN_4$	493.41
H5	3-[4-(1H-Benzimidazol-2-yl)phenyl]-2-methyl-2-{4-[2-(4-methylphenyl)-4-oxo-1,3-thiazolidin-3-yl]phenyl}-1,3-thiazolidin-4-one	$C_{33}H_{28}N_4O_2S_2$	576.75
H6	2-{4-[2-(4-Bromophenyl)-4-oxo-1,3-thiazolidin-3-yl]phenyl}-3-[4-(1H-benzimidazol-2-yl)phenyl]-2-methyl-1,3-thiazolidin-4-one	$C_{32}H_{25}BrN_4O_2S_2$	641.62

3.2. Spectroscopic Characterization of Compounds H2–H6

3.2.1. Characterization of H2 compound

The FTIR spectrum of H2 exhibited bands at 3328 and 3256 cm^{-1}, attributable to N–H stretching vibrations of the retained amino group and the benzimidazole N–H moiety. Aromatic C–H stretching appeared at 3114–3045 cm^{-1}. The band at 1607 cm^{-1} was assigned to the conjugated C=N stretching vibration, while the absence of a strong acetophenone

C=O absorption supported conversion of the ketone precursor into the ketimine. Additional band at 1582 from the aromatic and C–N framework.

^{1}H NMR spectra show exchangeable downfield resonance at δ 9.87 and 9.25 ppm, consistent with the amino NH_2 and benzimidazole N–H protons. Aromatic protons resonate in the δ 7.89–6.81 ppm region. The signal at δ 1.78 ppm is assign to the methyl group attached to the ketimine carbon, confirming retention of an acetophenone-derived methyl substituent after condensation.

In the ^{13}C NMR spectrum, the resonance at δ 161.30 ppm was assigned to the ketimine carbon. The benzimidazole and aromatic carbons appeared between δ 149.27 and 120.36 ppm, while the methyl carbon resonated at δ 29.27 ppm. Collectively, the FTIR and NMR data supported formation of H2 with one ketimine linkage and one retained amino group. Figures 1–3 show the FTIR, ^{1}H NMR, and ^{13}C NMR spectra of H2, respectively.

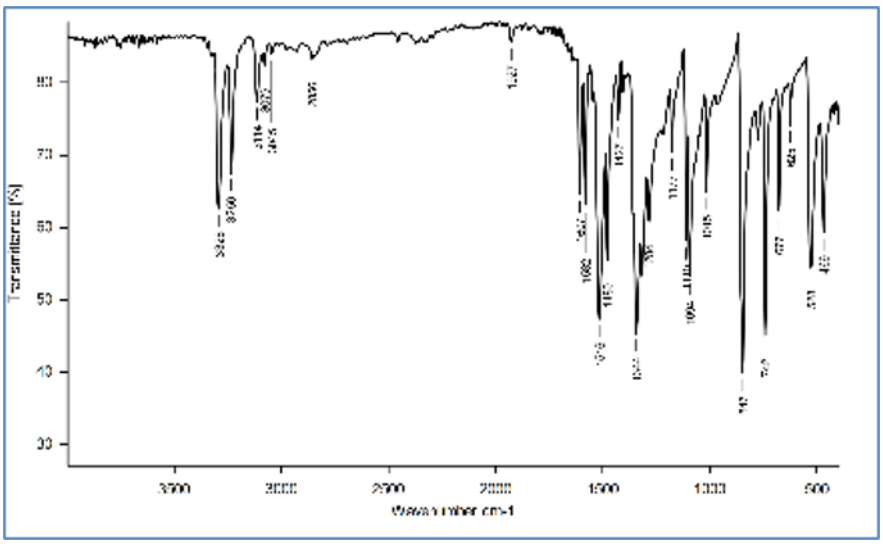

Figure 1 FTIR spectrum of compound H2.

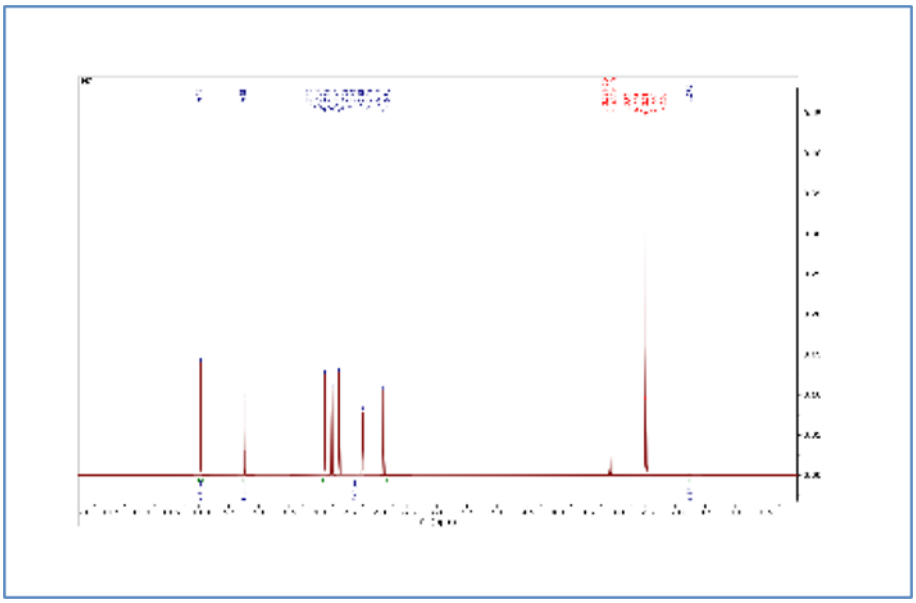

Figure 2 ^{1}H NMR spectrum of compound H2.

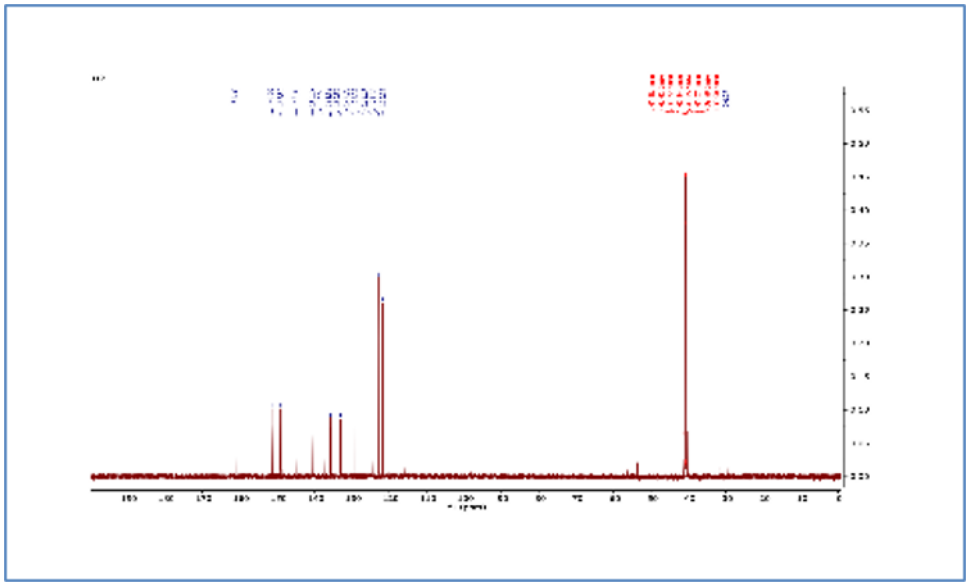

Figure 3 ^{13}C NMR spectrum of compound H2.

3.2.2. Characterization and Substituent Effects of H3 and H4

Condensation of the residual para-amino group of H2 with 4-methylbenzaldehyde or 4-bromobenzaldehyde afforded the bis-Schiff bases H3 and H4, respectively. For H3, the FTIR bands at 1586–1546 cm^{-1} were consistent with the conjugated C=N and aromatic framework. Aromatic and aliphatic C–H stretching bands appeared at approximately 3062 and 2926 cm^{-1}, respectively. The disappearance of the primary-amino stretching pattern observed for H2 supported completion of the second condensation.

The ^{1}H NMR spectrum of H3 displayed the benzimidazole N–H resonance at δ 9.98 ppm and aromatic/azomethine signals over δ 8.16–6.27 ppm. The resonances at δ 2.29 and 2.14 ppm were assigned to the para-methyl and ketimine-methyl groups, respectively. In the ^{13}C NMR spectrum, signal at δ 163.93 was assigned to the one chemically nonequivalent imine carbon and singles at δ 156.13 – 117.27 ppm for aromatic carbons , whereas the methyl carbons appeared at δ 25.50 and 20.17 ppm. These spectral features differentiated H3 from H2 and supported formation of the second imine linkage. Figs. 4–6 shown the FTIR, ^{1}H NMR, & ^{13}C NMR spectrum of H3, respective.

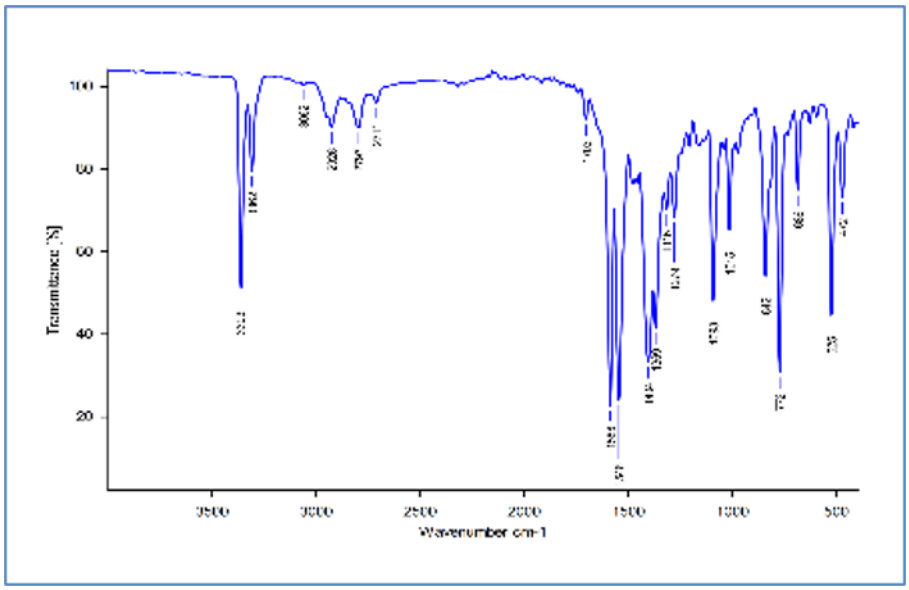

Figure 4 FTIR spectrum of compound H3.

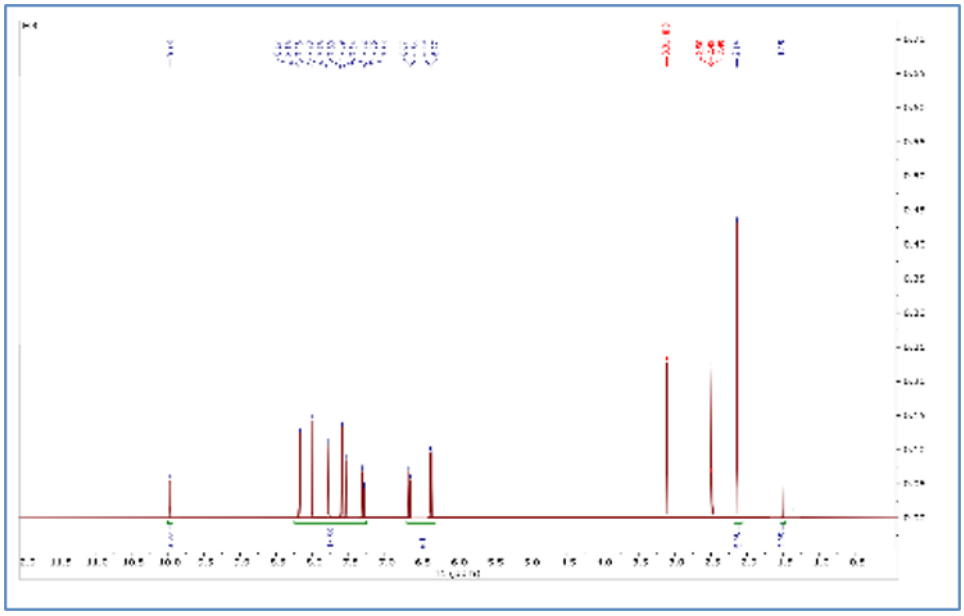

Figure 5 ^{1}H NMR spectrum of compound H3.

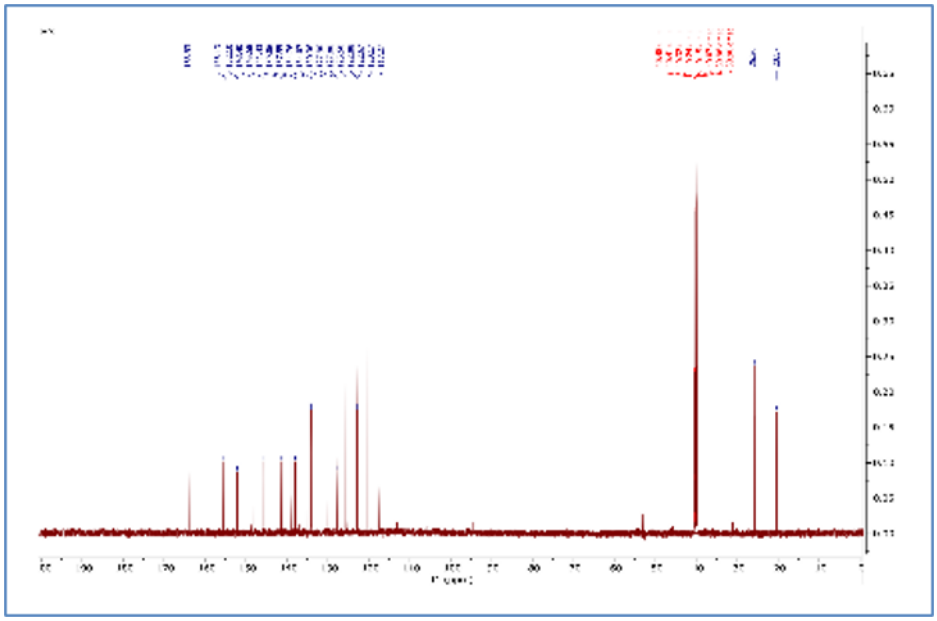

Figure 6 ^{13}C NMR spectrum of compound H3.

H4 contain ta same principal bis-imine framework as H3 but lack a para-methyl group & incorporate a para-bromophenyl ring. FTIR band at approximate 1598 & 1511 cm^{-1} support the conjugate C=N aromatic skeleton, while absorption in the 693–521 cm^{-1} region are consistent with the substitute aryl-bromide environment. ^{1}H NMR spectra of H4 show the benzimidazole N–H resonance at δ 9.83 ppm, aromatic/azomethine signal at δ 8.24–6.33 ppm, and the ketimine-methyl signal at δ 2.14 ppm. The ^{13}C NMR spectrum contained imine-carbon resonances at δ 158.85 ppm and the signals 156.32-117.83 ppm a methyl-carbon resonance at δ 21.63 ppm. The absence of a second aryl-methyl signal and the altered aromatic pattern distinguished H4 from H3. Figures 7–9 show the FTIR, ^{1}H NMR, and ^{13}C NMR spectra of H4, respectively.

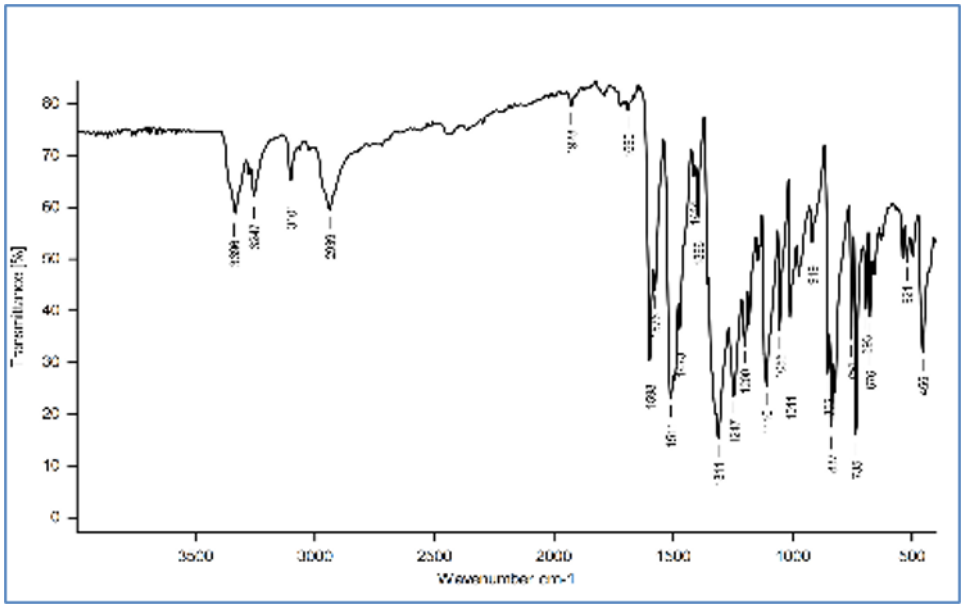

Figure 7 FTIR spectrum of compound H4.

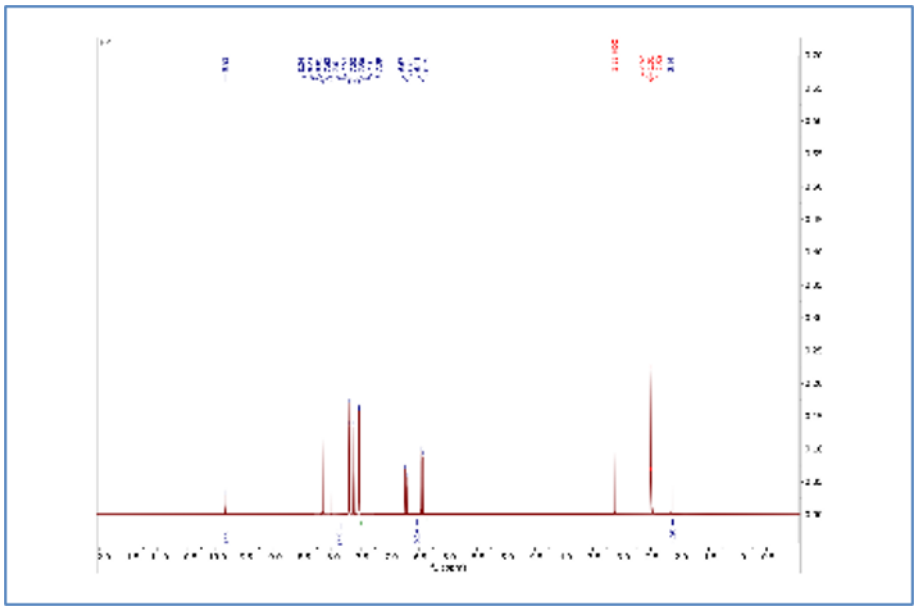

Figure 8 ^{1}H NMR spectrum of compound H4**.**

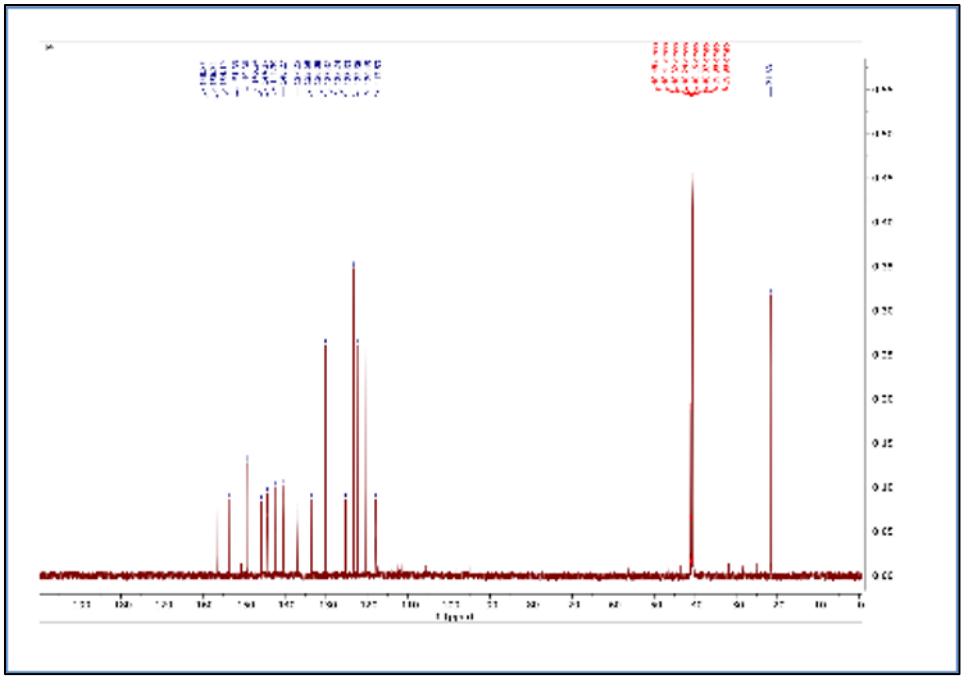

Figure 9 ^{13}C NMR spectrum of compound H4.

3.2.3. Characterization of the Bis(thiazolidin-4-one) Derivatives H5 and H6

The spectroscopic data of H5 were consistent with the formation of the proposed bis(thiazolidin-4-one) structure. Its FTIR spectrum exhibited two strong absorption band at approximately 1723 cm^{-1}, which were assigned to the carbonyl groups of the two chemically nonequivalent thiazolidin-4-one rings. This non-equivalence may be attributed to the different substitution environments of the rings: one ring contains a C2-methyl group derived from the ketimine moiety, whereas the other contains a para-tolyl substituent derived from the aldehyde moiety. Absorption bands within the 1547–1443 cm^{-1} region was associated with the conjugated aromatic framework and C=N and C–N vibrations, while the lower-frequency bands were consistent with C–S vibrations.

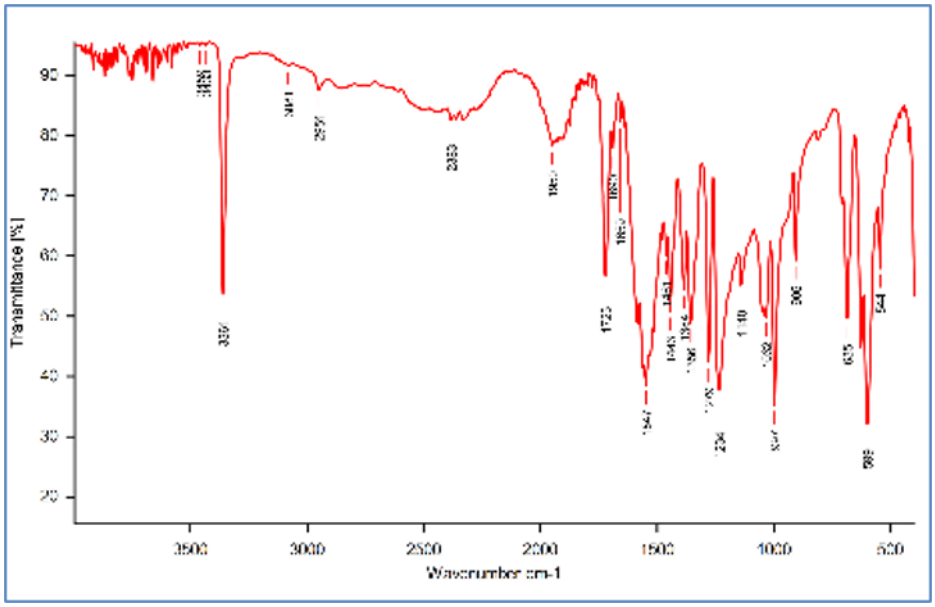

Figure 10 FTIR spectrum of compound H5.

The ^{1}H NMR spectrum of H5 displayed a downfield resonance at δ 10.97 ppm, assigned to the benzimidazole N–H proton. The aromatic protons and the thiazolidinone-ring methine proton appeared predominantly within the δ 7.79–6.49 ppm region. New resonances at δ 4.81 and 3.75 ppm were attributed to the chemically nonequivalent methylene

protons of the two thiazolidin-4-one rings. The signals at δ 2.07 and 1.73 ppm were assigned to the para-methyl and C2-methyl groups, respectively. The appearance of the thiazolidinone carbonyl absorptions and new aliphatic-ring proton signals, together with the disappearance of the characteristic azomethine-proton signal of H3, supported the proposed structure of H5. The FTIR and ^{1}H NMR spectra of H5 are presented in Figures 10 and 11, respectively.

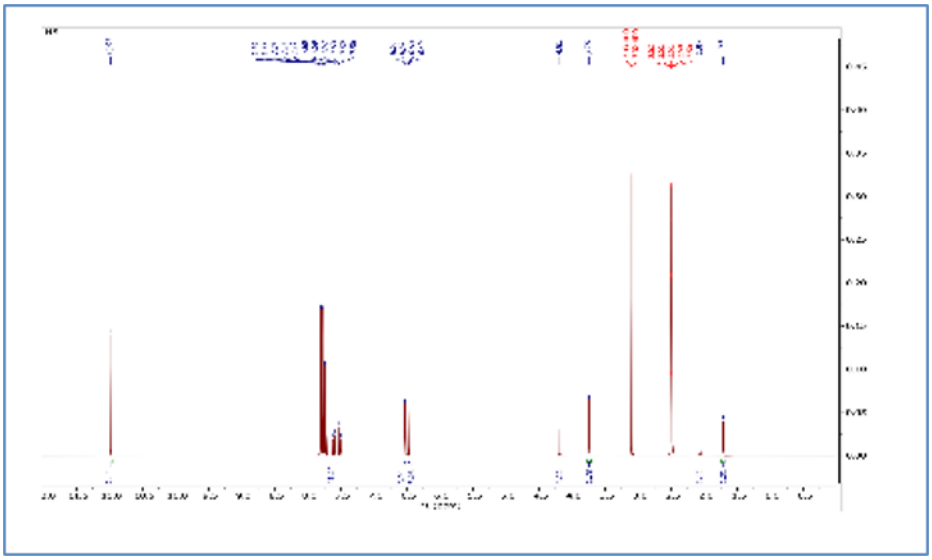

Figure 11 ^{1}H NMR spectrum of compound H5.

The FTIR spectrum of H6 exhibited a strong thiazolidinone carbonyl absorption at approximately 1746 cm^{-1} and additional bands in the 1605–1495 cm^{-1} region associated with conjugated aromatic and C–N/C=N vibrations. The ^{1}H NMR spectrum showed the benzimidazole N–H proton at δ 11.54 ppm, aromatic and ring-methine signals at δ 8.24–6.34 ppm, and new ring-methylene resonances at δ 4.24 and 4.14 ppm. The C2-methyl group resonated at δ 1.03 ppm. In contrast to H5, H6 lacked the para-methyl signal and exhibited the aromatic pattern expected for a para-bromophenyl substituent. These findings supported conversion of H5 into H6. Figures 12 and 13 show the FTIR and ^{1}H NMR spectra of H6, respectively.

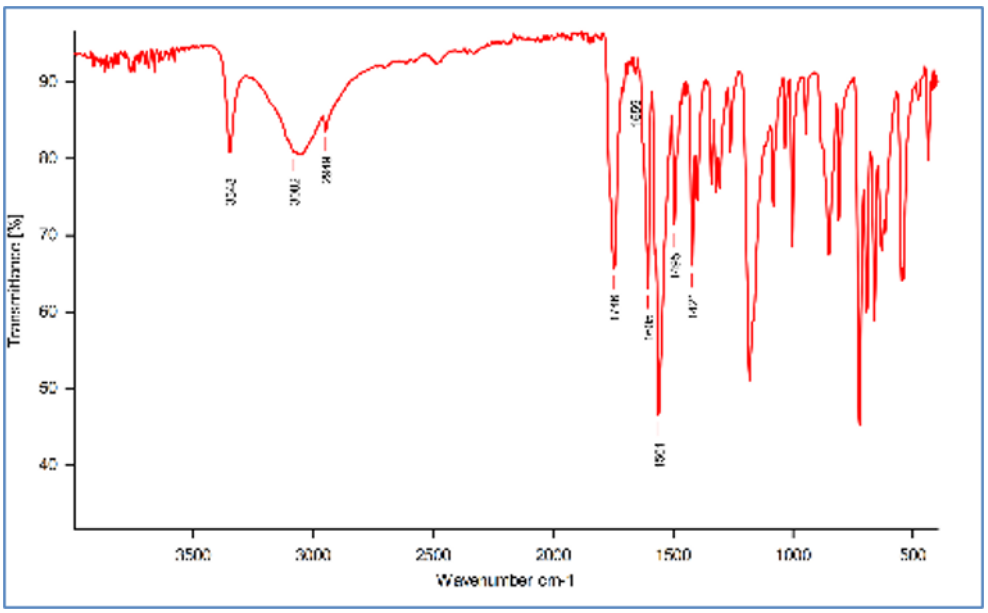

Figure 12 FTIR spectrum of compound H6.

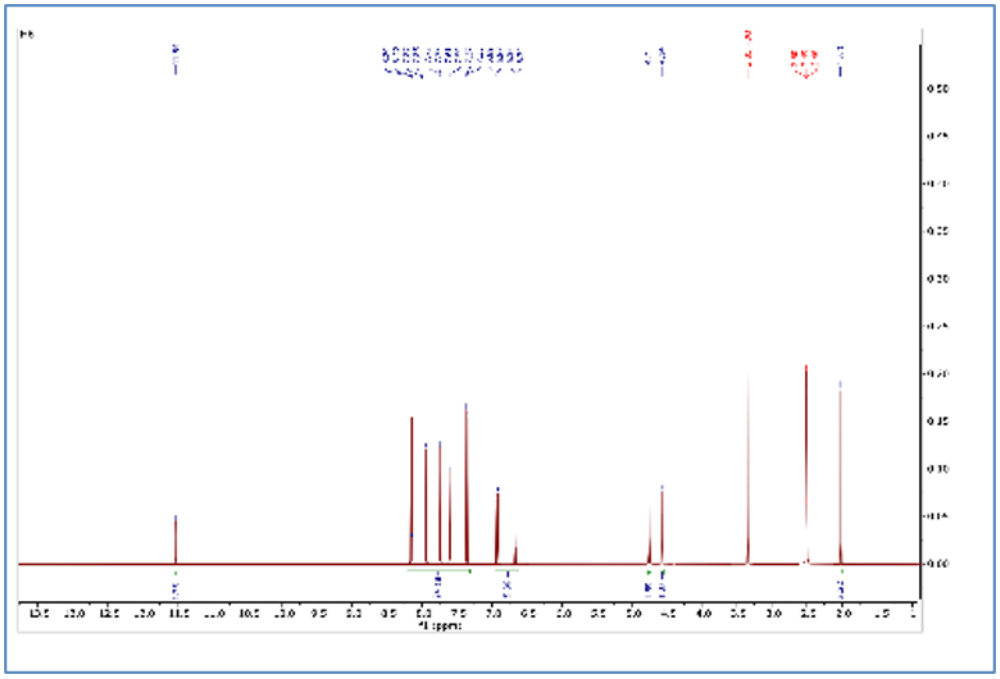

Figure 13 ^{1}H NMR spectrum of compound H6.

3.3. Evaluation of the biological activity of the prepared compounds

The measure inhibition-zone diameter of compounds H1–H6 are summarize in Table 2, and the comparative antibacterial response was shown in Figure 14. All compound inhibited both test organisms, with consistent larger zones against *S. aureus* than against *E. coli* under the apply condition.

Table 2 Measured inhibition-zone diameters of compounds H1–H6.

Compound	*E. coli (mm)*	*S. aureus (mm)*
H1	10	12
H2	14	16
H3	17	19
H4	19	21
H5	22	24
H6	24	26
DMSO	0	0

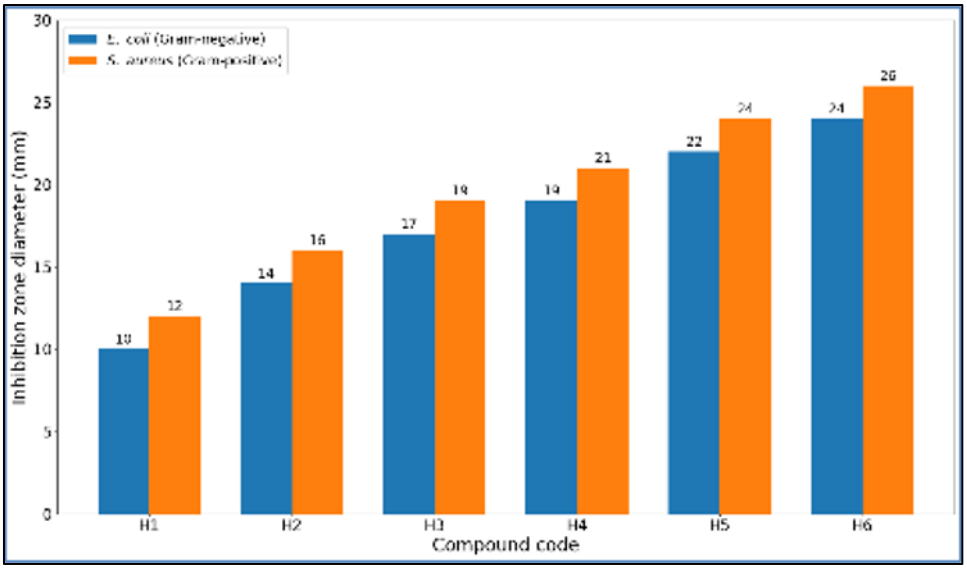

Figure 14 Measured inhibition-zone diameters of compounds H1–H6 against *E. coli* and *S. aureus*.

Among a test compounds, H6 exhibit the greatest antibacterial activities, producion inhibition zones of 24 mm against *E. coli* & 26 mm against *S. aureus*. H5 rank second, with inhibited zones of 22 and 24 mm, respective. The stronger response of the cyclize derivative relative to H3 and H4 indicates that conversion of the imine groups into thiazolidin-4-one rings is associate with enhance antibacterial activity.

H4 produced inhibition zones of 19 and 21 mm, whereas H3 produced zones of 17 and 19 mm against *E. coli* and *S. aureus*, respectively. The slightly greater response of the bromo-substituted analogue H4 than the methyl-substituted H3 suggests a substituent-dependent effect, potentially related to differences in electronic character, polarizability, and hydrophobic interactions.

H2 showed inhibition zones of 14 mm against *E. coli* and 16 mm against *S. aureus*, while H1 produced the smallest zones, 10 and 12 mm, respectively. Thus, extension of the molecular framework through successive imine formation increased activity relative to H1, and subsequent thiazolidin-4-one cyclization produced the largest inhibition zones.

Figure 15 Representative agar well diffusion plates for compound H1 against *E. coli* and *S. aureus*, with DMSO as the negative control.

DMSO produced no inhibition zone, confirming that the solvent did not contribute to the observed antibacterial response. The overall activity order was H6 > H5 > H4 > H3 > H2 > H1. The consistently larger zones against the Gram-positive *S. aureus* may be related to differences in cell-envelope structure compared with the outer-membrane barrier of Gram-negative *E. coli*. The observed structure–activity pattern is consistent with the reported antibacterial potential of benzimidazole, Schiff-base, halogenated, and thiazolidin-4-one frameworks [4,6,8,13,15].

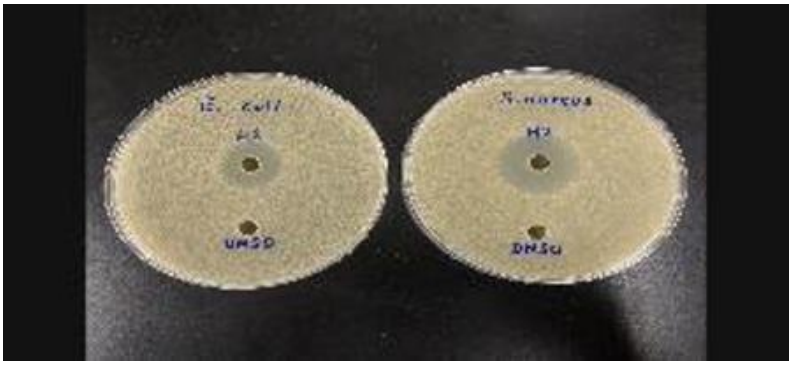

Figure 16 Representative agar well diffusion plates for compound H2 against *E. coli* and *S. aureus*, with DMSO as the negative control.

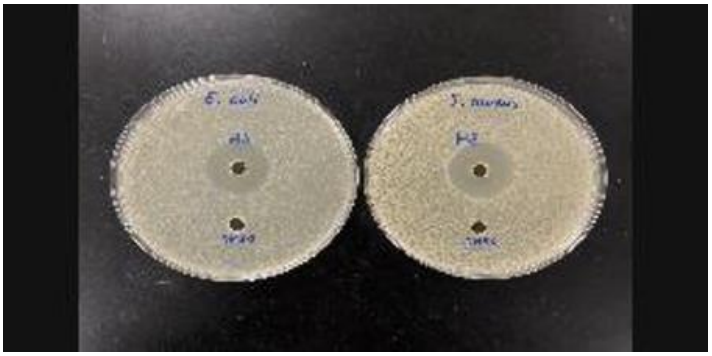

Figure 17 Representative agar well diffusion plates for compound H3 against *E. coli* and *S. aureus*, with DMSO as the negative control.

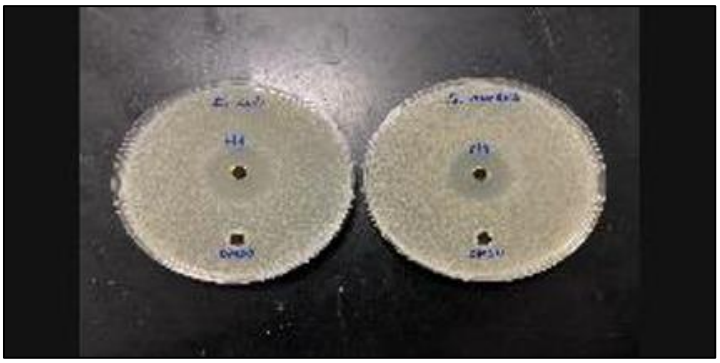

Figure 18 Representative agar well diffusion plates for compound H4 against *E. coli* and *S. aureus*, with DMSO as the negative control.

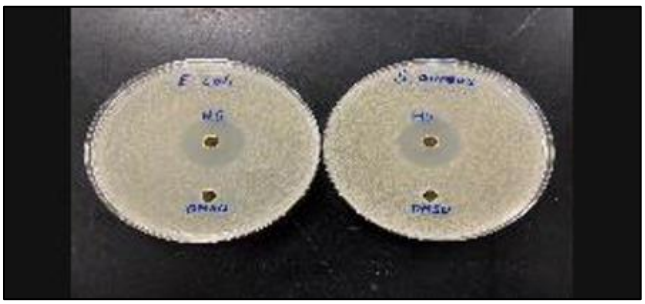

Figure 19 Representative agar well diffusion plates for compound H5 against *E. coli* and *S. aureus*, with DMSO as the negative control.

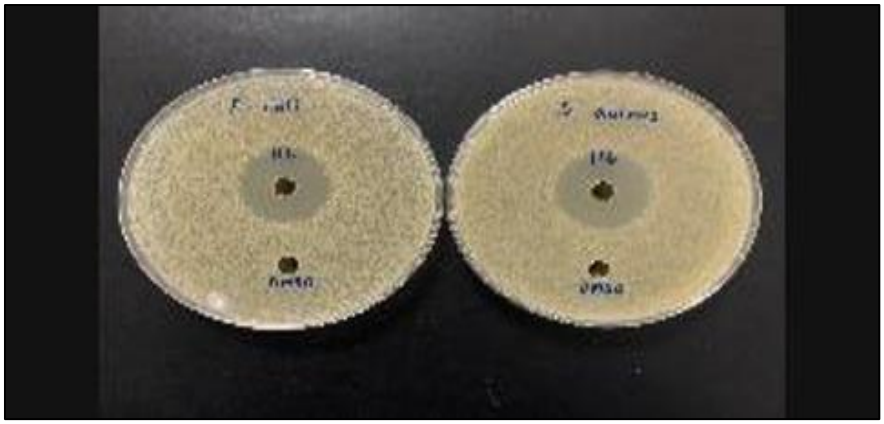

Figure 20 Representative agar well diffusion plates for compound H6 against *E. coli* and *S. aureus*, with DMSO as the negative control.

4. Conclusion

A series of benzimidazole-linked compounds H1–H6 was synthesized through sequential cyclocondensation, imine formation, and thiazolidin-4-one ring closure. The FTIR and NMR data showed systematic changes across the synthetic sequence, including retention and subsequent consumption of the amino group, formation of one and then two imine environments, and appearance of thiazolidinone carbonyl and saturated-ring signals after cyclization with thioglycolic acid. The methyl- and bromo-substituted branches followed the same overall pathway while exhibiting distinguishable substituent-dependent spectral features. In antibacterial assay, each compounds inhibit E. coli and S. aureus, & the activities increased from H1 and H2 to the bis-Schiff base and cyclize derivatives. H6 shown the largest inhibition zones, follow by H5, indicate that thiazolidin-4-one ring format & the para-bromo substituent are associate with enhanced antibacterial activities in this series. Overall, the combine spectroscopic and biological result support the successfully preparation of the propose benzimidazole–thiazolidin-4-one derivative and identify H5 and H6 as the most activation compounds investigated.

References

[1] Abd El-Lateef HM, Elbastawesy MAI, Abdelghani Ibrahim TM, Khalaf MM, Gouda M, Wahba MGF, et al. Design, synthesis, docking study, and antiproliferative evaluation of novel Schiff base-benzimidazole hybrids with VEGFR-2 inhibitory activity. Molecules. 2023;28(2):481. doi:10.3390/molecules28020481.

[2] Hussain R, Khan S, Ullah H, Ali F, Khan Y, Sardar A, et al. Benzimidazole-based Schiff base hybrid scaffolds: a promising approach to develop multi-target drugs for Alzheimer's disease. Pharmaceuticals (Basel). 2023;16(9):1278. doi:10.3390/ph16091278.

[3] Swikriti, Babbar R, Saini D, Rawat R, Chigurupati S, Felemban SG, et al. Design and synthesis of neoteric benzylidene amino-benzimidazole scaffolds for antioxidant and anti-inflammatory activity. Future Med Chem. 2023;15(10):813–828. doi:10.4155/fmc-2023-0058.

[4] Aroua LM, Alhag SK, Al-Shuraym LA, Messaoudi S, Mahyoub JA, Alfaifi MY, et al. Synthesis and characterization of different complexes derived from Schiff base and evaluation as a potential anticancer, antimicrobial, and insecticide agent. Saudi J Biol Sci. 2023;30(3):103598. doi:10.1016/j.sjbs.2023.103598.

[5] Celik I, Acar Cevik U, Kucukoglu K, Nadaroglu H, Bostanci HE, Isik A, et al. Design, synthesis, and molecular docking studies of benzimidazole-1,3,4-triazole hybrids as carbonic anhydrase I and II inhibitors. Chem Biol Drug Des. 2024;103(1):e14351. doi:10.1111/cbdd.14351.

[6] Khraisat LMAF, Sabuncuoglu S, Girgin G, Unsal Tan O. Synthesis and tyrosinase inhibitory activity of novel benzimidazole/thiazolidin-4-one hybrid derivatives. Chem Biodivers. 2024;21(2):e202301489. doi:10.1002/cbdv.202301489.

[7] Prakasha G, Revanasiddappa HD, Jayalakshmi B, Prabhakar BT, Shivamallu C, Viswanath PM, et al. Novel benzimidazole derived imine ligand and its Co(III) and Cu(II) complexes as anticancer agents: chemical synthesis, DFT studies, in vitro and in vivo biological investigations. Pharmaceuticals (Basel). 2023;16(1):125. doi:10.3390/ph16010125.

[8] Kumar D, Aggarwal N, Kumar H, Kapoor G, Deep A, Bibi S, et al. 2-Substituted-3-(5-substituted-1,3,4-oxadiazol/thiadiazol-2-yl) thiazolidin-4-one derivatives: synthesis, anticancer, antimicrobial, and antioxidant potential. Pharmaceuticals (Basel). 2023;16(6):805. doi:10.3390/ph16060805.

[9] Haque A, Khan MWA, Alenezi KM, Soury R, Khan MS, Ahamad S, et al. Synthesis, characterization, antiglycation evaluation, molecular docking, and ADMET studies of 4-thiazolidinone derivatives. ACS Omega. 2024;9(1):1810-1820. doi:10.1021/acsomega.3c08463.

[10] Ture A, Ergül M, Ergül M, Altun A, Kucukguzel I. Design, synthesis, and anticancer activity of novel 4-thiazolidinone-phenylaminopyrimidine hybrids. Mol Divers. 2021;25(2):1025-1050. doi:10.1007/s11030-020-10087-1.

[11] Alves JEF, de Oliveira JF, de Lima Souza TRC, de Moura RO, de Carvalho Junior LB, de Lima MCA, et al. Novel indole-thiazole and indole-thiazolidinone derivatives as DNA groove binders. Int J Biol Macromol. 2021;170:622-635. doi:10.1016/j.ijbiomac.2020.12.153.

[12] Haroon M, de Barros Dias MCH, da Silva Santos AC, Pereira VRA, Freitas LAB, Balbinot RB, et al. The design, synthesis, and in vitro trypanocidal and leishmanicidal activities of 1,3-thiazole and 4-thiazolidinone ester derivatives. RSC Adv. 2021;11(4):2487-2500. doi:10.1039/D0RA06994A.

[13] Lemilemu F, Bitew M, Demissie TB, Eswaramoorthy R, Endale M. Synthesis, antibacterial and antioxidant activities of thiazole-based Schiff base derivatives: a combined experimental and computational study. BMC Chem. 2021;15:67. doi:10.1186/s13065-021-00791-w.

[14] Buzun K, Kryshchyshyn-Dylevych A, Senkiv J, Roman O, Gzella A, Bielawski K, et al. Synthesis and anticancer activity evaluation of 5-[2-chloro-3-(4-nitrophenyl)-2-propenylidene]-4-thiazolidinones. Molecules. 2021;26(10):3057. doi:10.3390/molecules26103057.

[15] Tahmasvand R, Bayat P, Vahdaniparast SM, Dehghani S, Kooshafar Z, Khaleghi S, et al. Design and synthesis of novel 4-thiazolidinone derivatives with promising anti-breast cancer activity: synthesis, characterization, in vitro and in vivo results. Bioorg Chem. 2020;104:104276. doi:10.1016/j.bioorg.2020.104276.

[16] Sepehri S, Farhadi G, Maghbul M, Nasiri F, Faramarzi MA, Mahnam K, et al. A new route to the synthesis of 2-hydrazolyl-4-thiazolidinone hybrids, evaluation of alpha-glucosidase inhibitory activity and molecular modeling insights. Heliyon. 2024;10(16):e36408. doi:10.1016/j.heliyon.2024.e36408.

[17] Khan Y, Hussain R, Rehman W, Khan S, Maalik A, Iqbal T, et al. In-vitro and in-silico assessment of thiazole-thiazolidinone derivatives as selective inhibitors of urease and alpha-glucosidase. Future Med Chem. 2024;16(24):2627-2636. doi:10.1080/17568919.2024.2432303.

[18] Oubella A, Alossaimi MA, Riadi Y, Bhat MA, Bakheit AH, Taha ML, et al. Thiazolidinone-linked-1,2,3-triazoles with (R)-carvone as new potential anticancer agents. Future Med Chem. 2024;16(14):1449-1464. doi:10.1080/17568919.2024.2351287.

[19] Soni A, Kumar A, Kumar V, Rawat R, Eyupoglu V. Design, synthesis and evaluation of aminothiazole derivatives as potential anti-Alzheimer's candidates. Future Med Chem. 2024;16(6):513-529. doi:10.4155/fmc-2023-0290.

[20] Kumar G, Seboletswe P, Gcabashe N, Dhawan S, Manhas N, Bhargava G, et al. Rapid and environmentally-friendly synthesis of thiazolidinone analogues in deep eutectic solvent complemented with computational studies. ChemistryOpen. 2025;14(2):e202400198. doi:10.1002/open.202400198.

[21] Rekiba N, Benmohammed A, Khanoussi S, et al. Synthesis and characterization of novel thiazolidinones and thioxothiazolidinones derived from substituted indole. Molbank. 2021;2021(4):M1284. doi:10.3390/M1284.

[22] Nawaz M, Hayat S, Farooq U, Iqbal MA, Khalid SH, Nee TW, et al. Development of N-alkylated benzimidazole based cubosome hydrogel for topical treatment of burns. RSC Adv. 2024;14(44):32008-32020. doi:10.1039/D4RA04816D.

[23] Adnan S, Hassan K, Thamer H. Synthesis and identification some of heterocyclic compounds from imidazole derivatives. Iraqi National Journal of Chemistry. 2013;51:327–337.

[24] Belwal CK, Joshi KA. Synthesis and antifungal activity of some novel thiazolidinone derivatives of 4-(4-oxo-2-phenylthiazolidin-3-yl)benzoic acid. International Journal of ChemTech Research. 2012;4(4):1758–1764.